International Journal of Biochemistry and Cell Biology 111 (2019) 12–18

Contents lists available at ScienceDirect

International Journal of Biochemistry and Cell Biology

journal homepage: www.elsevier.com/locate/biocel

Hypoxia-induced autophagy promotes EGFR loss in specific cell contexts, which leads to cell death and enhanced radiosensitivity

Baocai Liu[1], Dongmei Han[1], Tingting Zhang, Guanghui Cheng*, Yinliang Lu, Jinbao Wang, Hongfu Zhao, Zhipeng Zhao

Department of Radiation Oncology, China-Japan Union Hospital of Jilin University, Changchun, 130033, China

ARTICLE INFO

Keywords:
Hypoxia
EGFR
Autophagy
Radiosensitivity

ABSTRACT

Treatment failure through radioresistance of tumors is associated with activation of the epidermal growth factor receptor (EGFR). Tumor cell proliferation, DNA-repair, hypoxia and metastases-formation are four mechanisms in which EGFR signaling has an important role. However, the effect of hypoxia on EGFR expression is still controversial. In this study, we demonstrated that hypoxia enhanced EGFR expression and sustained cell survival in SiHa, CAL 27 and A549 cells at both low and high cell desnities, while in MCF-7, MDA-MB-231 and HeLa cells, EGFR and cell survival were regulated by hypoxic treatment in a cell-density dependent manner: upregulated at low cell density and downregulated at high cell density. In MCF-7 and HeLa xenografts in nude mice, EGFR expression varied inversely with the pimonidazole level that was used as an indicator of hypoxia, accordant with the effect of hypoxia at high cell density *in vitro*. Hypoxia induced more remarkable cell autophagy at high cell density than at low cell density. Autophagy inhibitor 3MA, rather than proteasome inhibitor MG132 inhibited hypoxia-mediated EGFR loss and shifted cell death to cell survival in HeLa cells. The MCF7 cells' sensitivity to ionizing radiation (IR) under hypoxia was also conditional on the cell densities when the hypoxia treatment was introduced, inversely associated with the expression levels of EGFR. Altogether, hypoxia can decrease EGFR expression in some cell lines by enhancing autophagy at high cell density, leading to cell death and hypersensitivity to radiotherapy. This study may help to understand how hypoxia influences EGFR expression and radiosensitivity.

1. Introduction

Hypoxia is a common condition in the core of a wide range of solid tumors, which changes the characteristics of cancer cells and contributes to therapy resistance (Bertout et al., 2008; Semenza, 2012; Wilson and Hay, 2011). As tumor mass gradually grows, the oxygen concentration decreases as the distance of tumor cells from blood vessels increases, creating mild to severe hypoxia. In response to hypoxia, tumor cells will either become resistant to cancer therapies or undergo cell death.

One key factor that plays a central role in hypoxia induced resistance to tumor therapeutics such as radioresistance is the epidermal growth factor receptor (EGFR) (Sigismund et al., 2018), which is a membrane-associated receptor belonging to the ErbB/HER family of tyrosine kinases. Ligand binding, as well as various intrinsic or therapy-induced cellular stresses trigger EGFR trafficking and signaling, leading to a multitude of cellular responses including cell growth, proliferation, apoptosis, migration, and angiogenesis. Evidences have shown that hypoxic microenvironment in solid tumors not only translationally upregulates EGFR expression through HIF2α (Franovic et al., 2007), but also transactivates EGFR and triggers its internalization and non-degradative endosomal accumulation (Tan et al., 2016). In return, EGFR elicits the cellular response to hypoxia by activating its downstream signals such as ERK and AKT to promote the transcription of target genes, which are involved in EGFR-mediated cancer cell survival and therapy resistance (Guo et al., 2015; Yarden and Sliwkowski, 2001).

Although the expression of EGFR was reported to be upregulated by hypoxic conditions in breast, non-small-cell lung, cervical and head and neck cancers, some recent researches demonstrated that EGFR was significantly downregulated in hypoxic areas of the head and neck cancer (Mayer et al., 2016). EGFR signaling was found to be notably attenuated under hypoxic conditions (Garvalov et al., 2014; Nijkamp et al., 2011). The reason for these contradicting findings and the mechanism underlying hypoxia-mediated EGFR downregulation is still

* Corresponding author.
E-mail addresses: chengghcjuh@sina.com, chengguanghuifl@163.com (G. Cheng).
[1] These authors contributed equally to this work.

https://doi.org/10.1016/j.biocel.2018.09.013
Received 12 March 2018; Received in revised form 19 September 2018; Accepted 20 September 2018
Available online 29 September 2018
1357-2725/

unclear.

To elucidate whether the impact of hypoxia on EGFR expression is cell context specific or culturing density dependent, we chose the following cancer cells driven by EGFR and evaluated the EGFR expression after hypoxia treatment at different culturing density: a highly aggressive and poorly differentiated triple-negative breast cancer cell line MDA-MB-231, a well differentiated breast adenocarcinoma cell line MCF-7, a lung adenocarcinoma cell line A549, a squamous cervical carcinoma cell line SiHa, a cervical adenocarcinoma cell line HeLa, an oral adenosquamous carcinoma cell line CAL 27. Upregulation of EGFR was found in all examined cells when they were cultured at low cell density, while high cell density resulted in downregulation of EGFR in some of the cell lines. As an important mechanism that can be triggered by hypoxia for EGFR degradation and signaling limitation (So et al., 2014; Xu et al., 2016; Fang et al., 2015), autophagy was examined and proved to be associated with the cell density dependent EGFR loss under hypoxia. Radioresistance mediated by hypoxia was further assessed at different cell densities. This study may help to understand how hypoxia influences EGFR expression and the development of therapeutic methods.

2. Materials and methods

2.1. Cells and treatment

HeLa cells were grown in RPMI-1640 (Invitrogen, Grand Island, NY, USA) supplemented with 10% fetal bovine serum (Thermo Fisher Scientific, Waltham, MA, USA), MCF-7, MDA-MB-231, A549, SiHa and CAL 27 cells were cultured in DMEM (Invitrogen) supplemented with 10% fetal bovine serum (FBS, Thermo Fisher Scientific). The HeLa cell strain stably expressing GFP-LC3B (HeLa/GFP-LC3B) was a kind gift from Yingyu Chen (Peking University, Beijing, China). Cells were plated at 30% or > 90% confluency prior to exposure to hypoxia. Hypoxia treatment (12 or 24 h) was performed in a sealed humidified chamber containing 94% N_2, 5% CO_2 and 1% O_2. Oxygen concentrations in the hypoxia chamber were automatically adjusted by an electronic oxygen controller (ProOx Model 110, Biospherix, Redfield, NY, USA). Cells were treated with 10 mM 3-methyladenine (3-MA, Sigma-Aldrich, St. Louis, MO, USA) and 100 μM MG132 (Sigma-Aldrich) 1 h before hypoxia.

2.2. Cell viability assay

After hypoxic treatment, cells were harvested using trypsin, stained with 0.4% trypan blue (Beyotime Institute of Biotechnology, Jiangsu, China), and counted using a hemocytometer under phase contrast microscopy. Cell viability was calculated using the following formula: % viability = (unstained cell count/total cell count) × 100; % dead cell = (stained cell count/total cell count) × 100.

2.3. Western blot

Western blot was performed as previously described (Liu et al., 2015). Briefly, cells were lysed in RIPA lysis buffer (50 mM Tris-HCl, pH 7.4, 150 mM NaCl, 1% NP-40) supplemented with a 1% protease inhibitor cocktail (Roche, Basel, Switzerland). The protein concentrations were determined using BCA protein assays (Pierce, Rockford, IL, USA). The whole cell lysates were then fractionated using 10% or 15% SDS–PAGE gels and electrotransferred onto polyvinylidene difluoride membranes (GE, New York City, NY, USA). Antibodies used were as follows: GAPDH, cMet, EGFR, p62, AKT, phospho-AKT^{Ser473}, ERK, phospho-ERK$^{Thr202/Tyr204}$ (all from Cell Signaling Technology, Beverly, MA, USA), β-actin (Sigma-Aldrich). The protein bands were visualized using DyLight800-conjugated secondary antibody. Signals were detected by Odyssey Infrared Imager (LICOR Bioscience, Lincoln, NE, USA). The density of the bands was analyzed by ImageJ software (National Institutes of Health, Bethesda, MD, USA). The intensity of the target protein was normalized to the intensity of β-actin.

2.4. PCR and qPCR

The total RNAs were isolated from HeLa cells after hypoxia using TRIzol reagent (Invitrogen). Reverse transcription was performed according to standard protocols using a RevertAid™ II First Strand cDNA synthesis Kit (Thermo Fisher Scientific). Semiquantitative and quantitative PCR were performed as previously described (Liu et al., 2015). The primer for PCR of EGFR: F-5′-TCTTGCTGCTGGTGGTG-3′, R-5′-ATGCTGCGGTGTTTTCA-3′. The primer for qPCR of EGFR: F-5′-GCTTGCATTGATAGAAATGG-3′, R-5′-GTCGTCTATGCTGTCCTC-3′. GAPDH was amplified as an internal standard.

2.5. Confocal microscopy

Paraffin tissue sections were dewaxed, rehydrated and placed in 10 mmol/L citrate buffer (pH 6.0), and heated twice in a microwave oven for 5 min each. Sections were incubated with 3% H_2O_2 for 10 min, washed with PBS, blocked with 10% goat serum for 30 min. Sections were then incubated with the appropriate dilutions of primary antibodies at 4 °C overnight: anti-pimonidazole mouse antibody at 1:50 (Burlington, MA, USA), anti-EGFR rabbit antibody at 1:100 (Cell Signaling Technology), or anti-p62 rabbit antibody at 1:100 (Cell Signaling Technology), normal rabbit IgG as a negative control. FITC-conjugated rabbit anti-mouse IgG at 1:1000 (Cell Signaling Technology) and TRITC-conjugated goat anti-rabbit IgG at 1:1000 (Cell Signaling Technology) were served as secondary antibodies. The tissue sections were washed twice with PBS and stained with Hoechst 33342 (Cell Signaling Technology) before being imaged with an Ultra View VOX confocal laser scanning microscope (Perkin Elmer, Waltham, MA, USA).

2.6. Colony formation assay

Cells were plated at 30% or > 90% confluency prior to 24 h of hypoxia (1% O_2), and then radiated with different doses of radiation (0, 2, 4, 6 and 8 Gy). Subsequently, the cells were trypsinized and seeded in 6-well culture plates at the density of 1000 cells per well (in triplicate) under hypoxia. After 14 days, cells were fixed and stained with 0.5% crystal violet (Beyotime Institute of Biotechnology), and colonies of at least 50 cells were counted by GelCount (Oxford Optronix, Oxfordshire, Great Britain). Plating efficiency (PE) and survival fraction (SF) were calculated using the following formula: PE = colony numbers in sham-irradiated control/1000, SF = (colony numbers/1000)/PE. Survival curves were fitted in a multi-target single-hit model $[S = 1 - (1 - e^{-D/D0})^N]$ using Graphpad Prism 5.0 (Graphpad Software, San Diego, CA, USA).

2.7. Xenograft mouse model and treatment

All protocols regarding animals were reviewed and approved by the institutional Animal Research Ethics Board of Jilin University. Female BALB/c nude mice (6 weeks old) were maintained in a germ-free environment in the animal facility. The tumorigenesis assay was performed as previously described (Li et al., 2015). Briefly, HeLa or MCF-7 cells were trypsinized and suspended in PBS for subcutaneous injection. A total of 1×10^6 cells in 100 μL PBS were injected subcutaneously into the right axilla of nude mice (ten mice per group). Tumor diameters were measured with a caliper every 3 days, and tumor volumes were calculated according to length × width^2 × 0.5. When tumors reached 200 mm^3, mice were intraperitoneally injected with 60 mg/kg, pimonidazole (Hypoxyprobe-1, Hypoxyprobe, Burlington, MA, USA), which forms protein adducts under hypoxia. 90 min later, the mice were sacrificed and the tumor xenografts were excised and fixed in formalin for the immunofluorescence assay. At 200 magnification, 5–10 images per

section were randomly selected. All images were captured under consistent illumination and exposure for their respective stains. Hypoxic compartment was identified by pimonidazole staining, and cell death was assessed by TUNEL staining (Beyotime Institute of Biotechnology, Jiangsu, China).

2.8. Statistical analysis

The data were expressed as the mean ± SEM. Statistical analyses were performed using two-tailed Student's *t*-tests in Graphpad Prism 5.0 (Graphpad Software). Differences were considered significant when $P < 0.05$.

3. Results

3.1. Hypoxia leads to cell death and EGFR loss in a cell type and density dependent manner

It is generally accepted that the level of physiological hypoxia is about 1% O_2 (Franovic et al., 2007). However, tumor cells will experience more severe hypoxia in continuously proliferating and expanding tumor tissue. To simulate the *in vivo* growth patterns, we plated tumor cells at 30% and > 90% confluency prior to hypoxia (1% O_2), respectively. As hypoxia prevalently occurs in many solid epithelial tumors where EGFR overexpression is also a common feature (Schrevel et al., 2011; Baumann et al., 2007), we detected the effect of hypoxia on

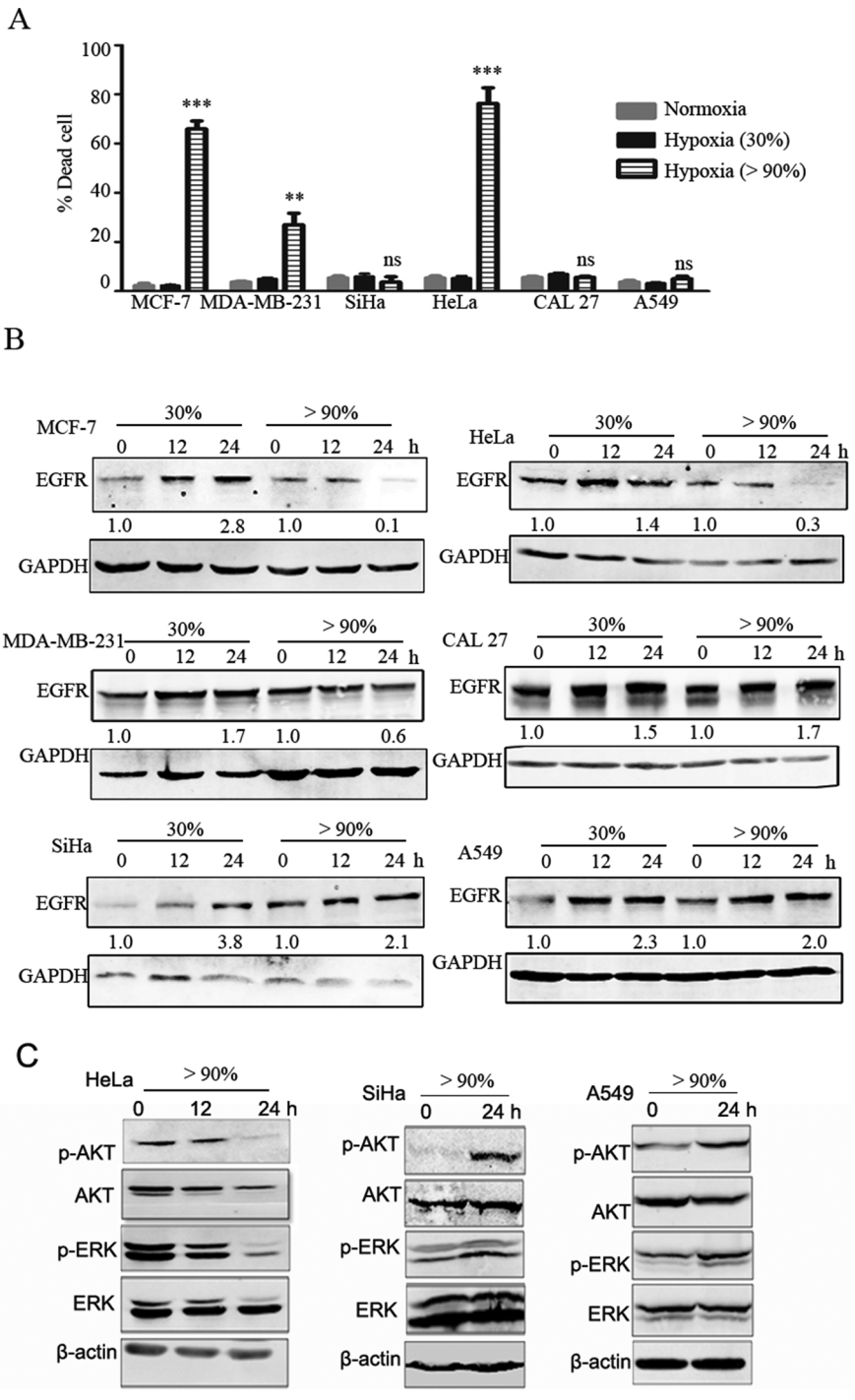

Fig. 1. Impact of hypoxia on cell death and EGFR expression at different cell densities. (A). The breast (MCF-7, MDA-MB-231), cervical (HeLa, SiHa), head and neck (CAL 27), and non small cell lung (A549) cancer cells were plated at low cell density (30%) or at high cell density (> 90%), and then treated with hypoxia for 24 h, the percentage of cell death was determined by 0.4% trypan blue (**$P < 0.01$, ***$P < 0.001$; ns, not significant). **(B)**. Cells were treated as in **(A)**, and the level of EGFR was detected by western blot, GAPDH was used as the internal standard. Data are representative of three independent experiments. **(C)**. HeLa, SiHa and A549 cells were plated at > 90% cell density, and cultured under hypoxia for indicated time points. Western blot analysis of the levels of EGFR, AKT, phospho-AKT, ERK, phospho-ERK and β-actin. Data are representative of three independent experiments. (For interpretation of the references to colour in this figure legend, the reader is referred to the web version of this article.)

cell survival and EGFR expression in a variety of breast (MCF-7, MDA-MB-231), cervical (HeLa, SiHa), head and neck (CAL 27), and non-small cell lung (A549) cancer cell lines. No obvious effect of hypoxia on cell survival was observed in all examined cells with 30% confluency (low cell density, LD). However at high cell density (HD, > 90% confluency), MCF-7, MDA-MB-231 and HeLa cells died severely after hypoxia treatment, while SiHa, CAL 27 and A549 cells retained their resistance against hypoxia-induced cell death (Figs. 1A and s1). Consistently, hypoxia enhanced EGFR expression in all examined cells at low cell density, as well as in high density of SiHa, CAL 27 and A549 cells, while in MCF-7, MDA-MB-231 and HeLa cells, EGFR was obviously down-regulated after 24 h of hypoxic treatment at high cell density (Fig. 1B). To confirm these results, we detected the effect of hypoxia on EGFR signaling pathways at HD, such as PI3K/AKT and Ras/ERK, and found that hypoxia decreased the phosphorylation of AKT and ERK in HeLa cells, but increased the phosphorylation of both kinases in SiHa and A549 cells (Fig. 1C). These results suggested that hypoxia leads to cell death and EGFR loss in a cell type and density dependent manner.

3.2. Hypoxia decreases EGFR expression level in vivo

Since hypoxia could lead to EGFR loss in MCF-7, MDA-MB-231and HeLa cells at high cell density *in vitro*, we subsequently used a xenograft model in BALB/c nude mice to test the *in vivo* effect of hypoxia on EGFR

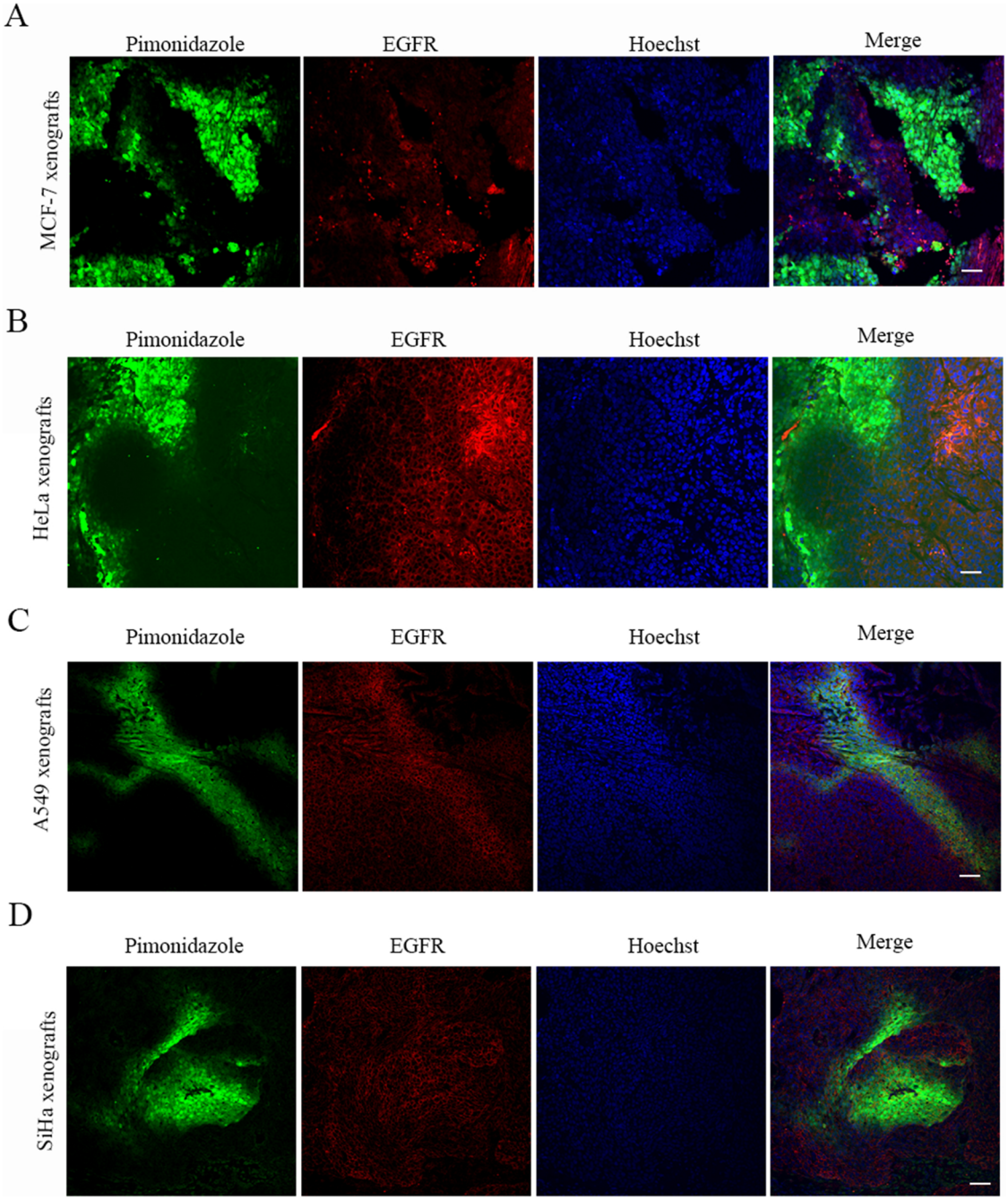

Fig. 2. Hypoxia decreases EGFR expression level *in vivo*. Nude mice bearing MCF-7, HeLa, A549 or SiHa xenografts were injected with pimonidazole. After 90 min, the mice were sacrificed, and tumors were fixed and stained with anti-pimonidazole (green) and anti-EGFR (red) and Hoechst (blue). Representative immunofluorescence images from 10 mice per group (MCF-7, HeLa, A549 and SiHa xenografts) were taken under a confocal microscope at × 200 and shown in **(A)–(D)**, respectively. Scale bars: 5 μm. (For interpretation of the references to colour in this figure legend, the reader is referred to the web version of this article.)

expression in these cells. MCF-7 or HeLa cells were injected subcutaneously into the right axilla of the nude mice, respectively. When tumors reached 200 mm^3, mice were intraperitoneally injected with pimonidazole, which can form protein adducts under hypoxia. 90 min after the injection, mice were euthanized. The distributions of hypoxia, EGFR and cell death were evaluated by staining with anti-pimonidazole and anti-EGFR antibodies and TUNEL, which were visualized under a confocal microscopy. As shown in Figs. 2A, B and s2, EGFR expression varied inversely with the levels of pimonidazole and cell death in both MCF-7 and HeLa xenografts. That is, the higher the hypoxia degree and cell death, the lower the expression of EGFR. These data suggested an accordant effect of hypoxia on EGFR expression and cell survival in MCF-7 and HeLa cells *in vivo* with that observed at high cell density *in vitro*. Furthermore, we ascertained that EGFR expression was positively correlated with the hypoxia level in A549 and SiHa xenograft tumors (Fig. 2C and D), consistent with our *in vitro* results.

3.3. Hypoxia-induced EGFR loss at high cell density is due to increased autophagy

Downregulation of EGFR could be due to decreased transcription or increased degradation. We then explored the potential mechanism underlying the high cell density-dependent hypoxia-induced EGFR loss in HeLa cells. By semiquantitative and quantitative PCR, we found no obvious change in EGFR mRNA levels during the hypoxia treatment (Fig. 3A, B), ruling out the impact of hypoxia on EGFR transcription. Then possible degradation pathways of EGFR were assessed. 3-methyladenine (3-MA), an autophagy/lysosome inhibitor and MG132, a

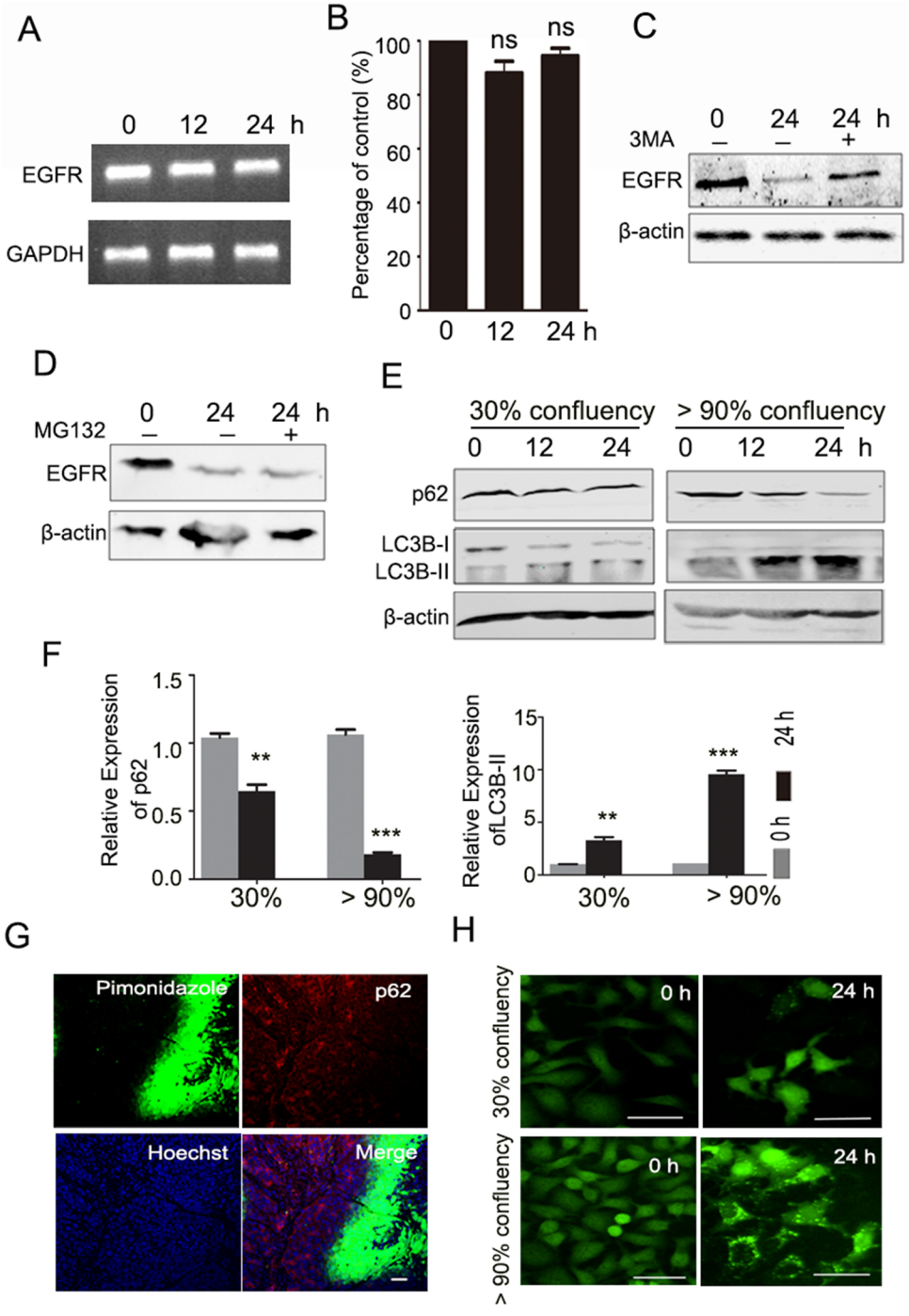

Fig. 3. Hypoxia-induced EGFR loss at high cell density is due to increased autophagy. HeLa cells were cultured at high cell density before hypoxia for indicated time points. EGFR mRNA expression was analyzed using semi-quantitative **(A)** and quantitative **(B)** PCR (ns, not significant). HeLa cells at high density were treated with 10 mM 3 MA **(C)** or 100 μM MG132 **(D)** starting 1 h before hypoxia. EGFR expression was detected by western blot. β-Actin was used as the internal standard. Data are representative of three independent experiments. **(E)**. HeLa cells were plated at low cell density or at high cell density, and then treated with hypoxia for 24 h. The levels of p62 and LC3B were analyzed by western blot. The grey densities of the target bands were analyzed by ImageJ software and normalized to the grey density of β-actin. The average relative grey density with the SEM from three independent experiments was shown in **(F)** ($^{**}P < 0.01$, $^{***}P < 0.001$). The *in vivo* correlation between hypoxia and p62 was analyzed using confocal microscopy. Representative immunofluorescence images from 10 mice were taken under a confocal microscope at × 200 and shown in **(G)**. Scale bars: 5 μm. **(H)**. HeLa cells stably expressing GFP-LC3B were treated as described in **(E)**. Representative confocal microscopy images of GFP-LC3B distribution were shown. Scale bars: 25 μm. (For interpretation of the references to colour in this figure legend, the reader is referred to the web version of this article.)

proteasome inhibitor were used respectively before hypoxia treatment at high cell density. The result showed that 3-MA, instead of MG132, significantly prevented EGFR loss and cell death induced by hypoxia (Fig. 3C, D), suggesting that autophagy-mediated lysosomal proteolysis might be the most likely mechanism for EGFR degradation in hypoxia.

Subsequently, hypoxia-induced autophagy was evaluated in HeLa cells at different cell densities. Western blot was performed to detect the levels of LC3B-II, an autophagy marker, and p62, an autophagy cargo that inversely correlates with the level of autophagy. As illustrated in Fig. 3E and F, LC3B-II level was more significantly increased by hypoxia in Hela cells at HD than in those at LD. Consistently, a more remarkable decrease of p62 level induced by hypoxia was found in HD cells than in LD cells. In the HeLa xenografts in nude mice, the hypoxic tumor regions also showed reduced p62 levels (Fig. 3G). We further monitored the distribution of GFP-LC3B in HeLa/GFP-LC3B cells under hypoxia using confocal microscopy, finding that there were much more GFP-LC3B puncta in HD cells as compared to LD cells (Fig. 3H). These results indicated that hypoxia induced a much higher degree of cell autophagy in HeLa cells at HD than at LD, which might contribute to the down-regulation of EGFR.

3.4. Hypoxia improves the sensitivity of cells undergoing hypoxia at HD to IR

EGFR upregulation has been thought as one of the determinant factors that contribute to hypoxia induced radioresistance in tumor therapeutics (Sigismund et al., 2018). Since we have demonstrated that hypoxia could lead to EGFR loss in MCF-7, MDA-MB-231 and HeLa cells at HD, the impact on radiosensitivity was further assessed. The MCF-7 cells undergoing 24 h of hypoxia at low or high cell density which resulted in increased or decreased EGFR expression respectively (as shown in Fig. 1B) were subjected to IR (0, 2, 4, 6, and 8 Gy), and their colony-forming abilities were then tested after reseeding the two groups of cells at the same density of 1000 cells/well in 6-well culture plates. As shown in Fig. 4A, two weeks after IR, the number of colonies formed by the HD group was obviously less than that of LD group. Likewise, the former showed a lower D0 value compared with the latter (1.58 *versus* 2.23) (Fig. 4B). Notably, the number of colonies formed from the low and high density of A549 cells had no obvious difference after two weeks of IR (Fig. s3). These results suggested that hypoxia treatment of cells at HD that might aggravate the hypoxia degree enhanced radiosensitivity instead of radioresistance, probably through downregulation of EGFR.

4. Discussion

In the present study, we demonstrated that EGFR was a switch regulating cell survival and death in hypoxia and associated with radiosensitivity. When EGFR expression was upregulated following hypoxia treatment, cells were destined to survive. Cells would undergo hypoxia-induced cell death and become more sensitive to IR, when EGFR was downregulated by hypoxia-mediated autophagy.

Most studies suggested that EGFR is upregulated in hypoxia (Nijkamp et al., 2013; Keulers et al., 2015; Tan et al., 2016). However, Heinz et al. recently established a novel method named multiplex immunofluorescence and single-cell segmentation, and demonstrated that EGFR expression was significantly downregulated with increasing distance from tumor vessels. Furthermore, they found that the phosphorylated ribosomal protein S6, a well-known downstream target of the EGFR-AKT signaling pathway, showed a preferential expression adjacent to blood vessels (Mayer et al., 2016). Kaanders et al. found that EGFR was present mainly in better oxygenated areas (Hoogsteen et al., 2012). Uhlen et al. demonstrated that EGFR expression was attenuated or missing in the distant cell layers of normal oral mucosa (Uhlén et al., 2015). In this study, we found that at low cell density, hypoxia obviously increased EGFR expression in all examined cells; while at high cell density, hypoxia led to EGFR loss in MCF-7, MDA-MB-231 and HeLa cells, but upregulated EGFR expression in A549, SiHa and CAL 27 cells. Based on accumulating evidences, we speculated that the effect of hypoxia on EGFR was correlated with cell density and histopathological patterns, which remains to be explored.

Autophagy is an important mechanism for EGFR degradation and signaling limitation. For example, the protein kinase CK2 inhibitor CX-4945 or the herbal plant derivative celastraol induced autophagic degradation of EGFR and consequently inhibited the survival of cancer cells (So et al., 2014; Xu et al., 2016). In the present study, we showed that hypoxia could induce autophagy in HeLa cells at HD to a high degree that might contribute to EGFR degradation. At the same time, PI3K/AKT and MAPK/ERK, two major downstream signaling pathways of EGFR, were obviously downregulated by hypoxia, which might impair the cell survival. We have confirmed that hypoxia enhanced EGFR expression in SiHa, CAL 27 and A549 cells, while in MCF-7, MDA-MB-231 and HeLa cells, EGFR was downregulated at high cell density. As hypoxia-induced autophagy is associated with the downregulation of EGFR, we speculated that different cell types with high cell density may have a distinct autophagic flux during hypoxia, which determines the level of EGFR in response to hypoxia.

Hypoxia-mediated EGFR downregulation is of great clinical significance. EGFR overexpression is generally believed to mediate radioresistance, and antibody-mediated EGFR downregulation could

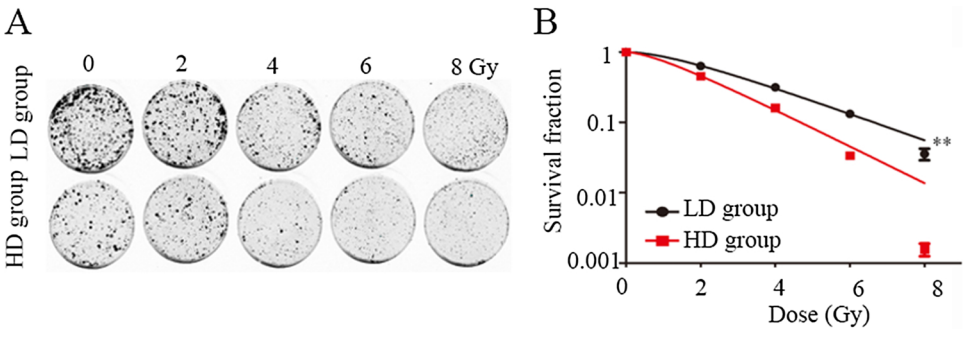

Fig. 4. Hypoxia improves the sensitivity of cells undergoing hypoxia at high cell density to IR. MCF-7 cells were plated at 30% (LD group) or > 90% confluency (HD group) prior to 24 h of hypoxia, and then radiated with different doses of radiation (0–8 Gy). Thereafter, the cells were seeded in 6-well culture plates at the density of 1000 cells per well under hypoxia. **(A)**. After 14 days of hypoxia, cells were fixed and stained with 0.5% crystal violet, and representative images of cell colonies formed by the LD group and HD group were shown by Odyssey Infrared Imager. Colonies with > 50 cells were quantified by GelCount. Survival curves fitted in a multi-target single-hit model $[S = 1 - (1 - e^{-D/D0})^N]$ using Graphpad Prism 5.0 were shown in **(B)** ($^{**}P < 0.01$).

lead to radiosensitization (Bonner et al., 2006; Santiago et al., 2010). In our experimental system, hypoxia-mediated EGFR loss at HD promoted the cancer cells' death, and the remaining cells became more sensitive to radiotherapy compared with cells undergoing hypoxia at LD, where EGFR was upregulated. Based on our data, we hypothesized that further exacerbated hypoxia mimicked by high culturing density might improve radiosensitivity instead of radioresistance, probably through downregulation of EGFR. We will examine additional cell types and conduct clinical trials to further support our conclusion.

In addition to EGFR, other receptor tyrosine kinases (RTKs) also play roles in the tumor progression under hypoxia, especially hepatocyte growth factor receptor (cMet) (Le et al., 2012). Our data suggested that unlike EGFR, hypoxia had no apparent effect on cMet expression (data not shown), suggesting that hypoxia play a receptor-specific role in regulation of the RTKs' expression. Taken together, in this study, our results suggested that under hypoxia, cell type and density determine the change of EGFR expression, which regulates cell survival and radiosensitivity.

Conflict of interest

The authors declare no conflicts of interest.

Acknowledgements

This work was supported by grantsfrom the National Natural Science Foundation of China (81703034, 31600679), the Project of Science and Technology Department of Jilin Province (20090458), the Project of Health and Family Planning Commission of Jilin Province (2014ZC054), the Bethune Special Research of Science and Technology Department of Jilin Province (20160101079JC), and the Horizontal Project of Jilin University (2015373).

Appendix A. Supplementary data

Supplementary material related to this article can be found, in the online version, at doi:https://doi.org/10.1016/j.biocel.2018.09.013.

References

Baumann, M., Krause, M., Dikomey, E., et al., 2007. EGFR-targeted anti-cancer drugs in radiotherapy: preclinical evaluation of mechanisms. Radiother. Oncol. 83, 238–248.
Bertout, J.A., Patel, S.A., Simon, M.C., 2008. The impact of O_2 availability on human cancer. Nat. Rev. Cancer 8, 967–975.
Bonner, J.A., Harari, P.M., Giralt, J., et al., 2006. Radiotherapy plus cetuximab for squamous-cell carcinoma of the head and neck. N. Engl. J. Med. 354, 567–578.
Fang, Y., Tan, J., Zhang, Q., 2015. Signaling pathways and mechanisms of hypoxia-induced autophagy in the animal cells. Cell Biol. Int. 39, 891–898.
Franovic, A., Gunaratnam, L., Smith, K., et al., 2007. Translational up-regulation of the EGFR by tumor hypoxia provides a nonmutational explanation for its overexpression in human cancer. Proc. Natl. Acad. Sci. U. S. A. 104, 13092–13097.
Garvalov, B.K., Foss, F., Henze, A.T., et al., 2014. PHD3 regulates EGFR internalization and signalling in tumours. Nat. Commun. 5, 5577.
Guo, G., Gong, K., Wohlfeld, B., et al., 2015. Ligand-independent EGFR signaling. Cancer Res. 75, 3436–3441.
Hoogsteen, I.J., Marres, H.A., van den Hoogen, F.J., et al., 2012. Expression of EGFR under tumor hypoxia: identification of a subpopulation of tumor cells responsible for aggressiveness and treatment resistance. Int. J. Radiat. Oncol. Biol. Phys. 84, 807–814.
Keulers, T.G., Schaaf, M.B., Peeters, H.J., et al., 2015. GABARAPL1 is required for increased EGFR membrane expression during hypoxia. Radiother. Oncol. 116, 417–422.
Le, Q.T., Fisher, R., Oliner, K.S., et al., 2012. Prognostic and predictive significance of plasma HGF and IL-8 in a phase III trial of chemoradiation with or without tirapazamine in locoregionally advanced head and neck cancer. Clin. Cancer Res. 18, 1798–1807.
Li, T., Cheng, Y., Wang, P., et al., 2015. CMTM4 is frequently downregulated and functions as a tumour suppressor in clear cell renal cell carcinoma. J. Exp. Clin. Cancer Res. 34, 122.
Liu, B., Su, Y., Li, T., et al., 2015. CMTM7 knockdown increases tumorigenicity of human non-small cell lung cancer cells and EGFR-AKT signaling by reducing Rab5 activation. Oncotarget 6, 41092–41107.
Mayer, A., Zahnreich, S., Brieger, J., et al., 2016. Downregulation of EGFR in hypoxic, diffusion-limited areas of squamous cell carcinomas of the head and neck. Br. J. Cancer 115, 1351–1358.
Nijkamp, M.M., Hoogsteen, I.J., Span, P.N., et al., 2011. Spatial relationship of phosphorylated epidermal growth factor receptor and activated AKT in head and neck squamous cell carcinoma. Radiother. Oncol. 101, 165–170.
Nijkamp, M.M., Span, P.N., Bussink, J., et al., 2013. Interaction of EGFR with the tumour microenvironment: implications for radiation treatment. Radiother. Oncol. 108, 17–23.
Santiago, A., Eicheler, W., Bussink, J., et al., 2010. Effect of cetuximab and fractionated irradiation on tumour micro-environment. Radiother. Oncol. 97, 322–329.
Schrevel, M., Gorter, A., Kolkman-Uljee, S.M., et al., 2011. Molecular mechanisms of epidermal growth factor receptor overexpression in patients with cervical cancer. Mod. Pathol. 24, 720–728.
Semenza, G.L., 2012. Hypoxia-inducible factors: mediators of cancer progression and targets for cancer therapy. Trends Pharmacol. Sci. 33, 207–214.
Sigismund, S., Avanzato, D., Lanzetti, L., 2018. Emerging functions of the EGFR in cancer. Mol. Oncol. 12, 3–20.
So, K.S., Kim, C.H., Rho, J.K., et al., 2014. Autophagosome-mediated EGFR down-regulation induced by the CK2 inhibitor enhances the efficacy of EGFR-TKI on EGFR-mutant lung cancer cells with resistance by T790M. PLoS One 9, e114000.
Tan, X., Lambert, P.F., Rapraeger, A.C., et al., 2016. Stress-induced EGFR trafficking: mechanisms, functions, and therapeutic implications. Trends Cell Biol. 26, 352–366.
Uhlén, M., Fagerberg, L., Hallström, B.M., et al., 2015. Proteomics. Tissue-based map of the human proteome. Science 347, 1260419.
Wilson, W.R., Hay, M.P., 2011. Targeting hypoxia in cancer therapy. Nat. Rev. Cancer 11, 393–410.
Xu, S.W., Law, B.Y., Mok, S.W., et al., 2016. Autophagic degradation of epidermal growth factor receptor in gefitinib-resistant lung cancer by celastrol. Int. J. Oncol. 49, 1576–1588.
Yarden, Y., Sliwkowski, M.X., 2001. Untangling the ErbB signalling network. Nat. Rev. Mol. Cell Biol. 2, 127–137.